Supplementary information

Efficient Removal of Sr^{2+} by a Layered Metal Sulfide $K_{1.36}Cd_{1.12}Bi_{2.80}S_6$ via Ion Exchange

Lenian Qu[1,2,3], Yuxin Fang[1,3,4], Ziyi Wan[1,3,4], Meiling Feng[1,2,3,*] and Xiaoying Huang[1,2,3]

[1] State Key Laboratory of Structural Chemistry, Fujian Institute of Research on the Structure of Matter, Chinese Academy of Sciences, Fuzhou 350002, China;
qulenian@fjirsm.ac.cn (L.Q.); fangyuxin@fjirsm.ac.cn (Y.F.); wanziyi@fjirsm.ac.cn (Z.W.);
xyhuang@fjirsm.ac.cn (X.H.)

[2] University of Chinese Academy of Sciences, Beijing 100049, China

[3] Fujian College, University of Chinese Academy of Sciences, Fuzhou 350002, China

[4] College of Chemistry, Fuzhou University, Fuzhou 350116, China

* Correspondence: fml@fjirsm.ac.cn; Tel.: +86-591-63173146

1. Equations

This study systematically investigated the adsorption behaviour of KCBS towards Sr^{2+} using multiple parameters and models, employing the following equations.

(1) Adsorption capacity

$$q = \frac{(C_0 - C_e)V}{m} \qquad \text{(Eq. S1)}$$

q denotes the mass of metal ions adsorbed per unit mass of adsorbent from the solution, where C_0 (mg·L^{-1}) and C_e (mg·L^{-1}) represent the initial concentration and equilibrium concentration respectively, V (mL) is the volume of the solution, and m (g) is the mass of the adsorbent.

(2) Adsorption isotherm models

Langmuir model

$$q_e = q_m \frac{bC_e}{1+bC_e} \qquad \text{(Eq. S2)}$$

Freundlich model

$$q_e = K_F C_e^{\frac{1}{n}} \qquad \text{(Eq. S3)}$$

Langmuir-Freundlich model

$$q_e = q_m \frac{(bC_e)^{\frac{1}{n}}}{1+(bC_e)^{\frac{1}{n}}} \qquad \text{(Eq. S4)}$$

The Langmuir, Freundlich, and Langmuir-Freundlich models were employed to fit the adsorption isotherms, thereby determining the maximum adsorption capacity (q_m·mg·g^{-1}) and elucidating the adsorption mechanism. b and n denote the adsorption constants.

(3) Removal rate

$$R = \frac{(C_0 - C_e)}{C_0} \times 100\% \qquad \text{(Eq. S5)}$$

R denotes the removal efficiency of the adsorbent for the target object.

(4) Kinetics models

Pseudo-first-order kinetics model

$$\ln (q_e - q_t) = \ln q_e - k_1 t \qquad \text{(Eq. S6)}$$

Pseudo-second-order kinetic model

$$\frac{t}{q_t} = \frac{1}{k_2 q_e^2} + \frac{1}{q_e} t \qquad \text{(Eq. S7)}$$

Where q_e (mg·g^{-1}) and q_t (mg·g^{-1}) are the ion exchange capacities at equilibrium and t (min), respectively. k_1 (min^{-1}) is the pseudo-first-order rate constants of kinetics models. And k_2 (g mg^{-1}·min^{-1}) is the pseudo-second-order rate constants of kinetics models.

(5) Distribution coefficient

$$K_d = \frac{V}{m} \frac{(C_0 - C_e)}{C_e} \qquad \text{(Eq. S8)}$$

The distribution coefficient K_d (mL·g^{-1}) is commonly employed to evaluate the affinity of ion exchange materials for target ions.

(6) The thermodynamic equation

$$\Delta G^0 = -RT \ln K_C \qquad \text{(Eq. S9)}$$

$$\Delta G^0 = \Delta H^0 - T\Delta S^0 \qquad \text{(Eq. S10)}$$

$$\ln K_C = -\frac{\Delta H^0}{RT} + \frac{\Delta S^0}{R} \qquad \text{(Eq. S11)}$$

The Gibbs free energy change (ΔG^0) of the system was calculated using Eq. S9. The relationship between ΔG^0, the enthalpy change (ΔH^0), and entropy change (ΔS^0) is described by Eq. S10. Eq. S11, known as the Van't Hoff equation, is derived from Eqs. S9 and S10. Here, K_C represents the equilibrium constant, R is the ideal gas constant (8.314 J·mol^{-1}·K^{-1}), and T is the absolute temperature (K).

(7) Leaching rate (R_L)

$$R_L = \frac{C_p}{C_t} \times 100\% \qquad \text{(Eq. S12)}$$

where R_L(%) is the leaching rate, C_p (mg·L^{-1}) is the concentration of Cd or Bi ions in the solution after soaking the samples, and C_t (mg·L^{-1}) is the theoretical concentration of Cd or Bi ions when the sample is completely dissolved in the solution.

(8) Separation factor

$$SF = \frac{K_d^A}{K_d^B} \qquad \text{(Eq. S13)}$$

The separation factor (SF) is employed to evaluate the selectivity of an adsorbent towards a particular ion.

(9) Desorption efficiency

$$E = \frac{C_e^{de} V_{de}}{m_2(m^{ad}/m_1)} \times 100\% \qquad \text{(Eq. S14)}$$

C_e^{de} (mg·L^{-1}) and V_{de} (mL) denote the concentration of Sr^{2+} in the desorption solution and the volume of the desorption solution used, respectively. m^{ad} (mg) represents the mass of Sr^{2+} fixed during the adsorption stage. Due to inevitable solid losses during the cyclic process—arising from washing, drying, and PXRD characterization—the solid mass was precisely weighed before each experimental step. Here, m_1 (mg) refers to the mass of the solid sample after Sr^{2+} adsorption, and m_2 (mg) is the mass of solid actually used in the desorption experiment. The desorption efficiency (E^{Sr}) was calculated based on the adsorbed amount of Sr^{2+} corresponding to m_2, thereby accurately evaluating the release performance of the measurable portion of the material.

2. Additional Results and Discussion

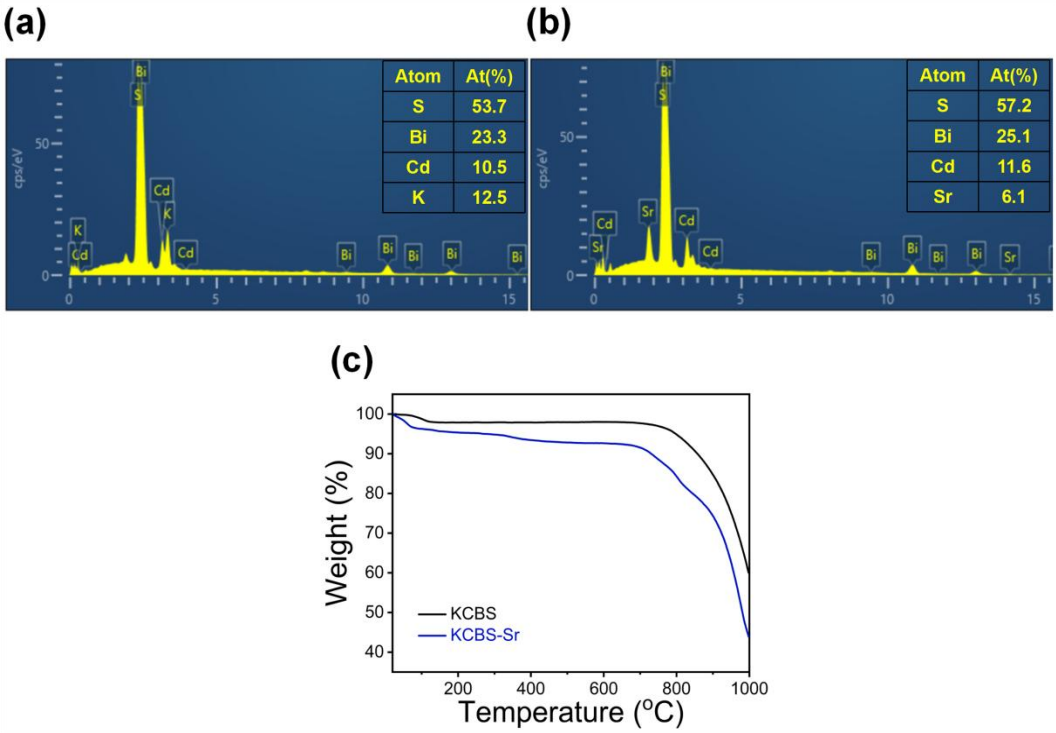


Figure S1. EDS analysis results of (a) KCBS and (b) KCBS-Sr. (c) TGA curves for KCBS and KCBS-Sr.

Table S1. Crystallographic data and structural refinements for compounds KCBS

Compound	KCBS
Empirical formula	$K_{1.36}Cd_{1.12}Bi_{2.80}S_6$
Formula weight	956.57
Temperature (K)	100(2)
Crystal system	hexagonal
Space group	$P6_3/mmc$
a (Å)	3.98290(10)
b (Å)	3.98290(10)
c (Å)	23.2854(6)
V (Å^3)	319.899(18)
Z	1
ρ_{calcd} (g/cm^3)	4.965
μ (MoK_α) / (mm^{-1})	41.595
F(000)	408.0
Crystal size (mm^3)	0.20 × 0.15 × 0.05
λ(MoK_α) (Å)	0.71073
2θ range (°)	3.948 to 61.61
Index ranges	$-5 \le h \le 5$, $-5 \le k \le 5$, $-32 \le l \le 31$
Reflections collected	6363
Independent reflections	232 [R_{int} = 0.0644, R_{sigma} = 0.0165]
Data/restraints/parameters	232/18/25
Goodness of fit on F^2	1.181
Final R indexes $I > 2\sigma(I)$	R_1[a] = 0.0293, wR_2[b]= 0.0910
Final R indexes	R_1[a] = 0.0311, wR_2[b] = 0.0923
Largest diff. peak/hole / e Å^{-3}	1.86/-1.33
CCDC number	2521470

[a] $R_1 = \sum \| F_o \| - \| F_c \| / \sum | F_o |$, [b] $wR_2 = [\sum w(F_o^2 - F_c^2)^2 / \sum w(F_o^2)^2]^{1/2}$.

Table S2. Selected bond lengths (Å) for KCBS.

Bi(1)-S(1)#1	2.922(3)	Bi(1)-S(2)#3	2.702(4)	Cd(1)-S(2)#1	2.754(16)	S(2)-K(2)#8	3.282(5)
Bi(1)S(1)#2	2.922(3)	Cd(1)-S(1)#1	2.863(17)	Cd(1)-S(2)#3	2.754(16)	S(2)-K(2)	3.282(5)
Bi(1)-S(1)	2.922(3)	Cd(1)-S(1)	2.863(17)	S(2)-K(1)#6	3.238(14)	S(2)-K(2)#7	3.282(5)
Bi(1)-S(2)#1	2.702(4)	Cd(1)-S(1)#2	2.863(17)	S(2)-K(1)#5	3.238(13)	S(2)-K(2)#9	3.282(5)
Bi(1)-S(2)	2.702(4)	Cd(1)-S(2)	2.754(16)	S(2)-K(1)#7	3.238(14)	S(2)-K(2)#6	3.282(5)

Symmetry transformations used to generate equivalent atoms: 1# 1+*x*,+*y*,+*z*; 2# 1+*x*,1+*y*,+*z*; 3# +*x*,-1+*y*,+*z*; 5# 1+*y*-*x*,1-*x*,+*z*; 6# +*x*,1+*y*,+*z*; 7# -*y*,+*x*-*y*,+*z*; 8# +*y*-*x*,1-*x*,+*z*; 9# 1-*y*,1+*x*-*y*,+*z*; 10# +*y*-*x*,-*x*,+*z*; 11# 1+*y*-*x*,-*x*,+*z*

Table S3. Selected bond angles (°) for KCBS.

S(1)-Bi(1)-S(1)#1	85.93(12)	S(2)#5-Bi(1)-S(1)	89.37(5)	S(2)-Cd(1)-S(1)#1	176.8(10)
S(1)-Bi(1)-S(1)#2	85.93(12)	S(2)-Bi(1)-S(1)#2	89.37(5)	S(2)#1-Cd(1)-S(1)#1	176.8(10)
S(1)#1-Bi(1)-S(1)#2	85.93(12)	S(2)#1-Bi(1)-S(2)#5	94.96(16)	S(2)#5-Cd(1)-S(1)#1	89.57(6)
S(2)#1-Bi(1)-S(1)#1	89.37(5)	S(2)#1-Bi(1)-S(2)	94.96(16)	S(2)#5-Cd(1)-S(1)	89.57(6)
S(2)#5-Bi(1)-S(1)#2	173.6(2)	S(2)#5-Bi(1)-S(2)	94.96(16)	S(2)#1-Cd(1)-S(1)#2	89.57(6)
S(2)-Bi(1)-S(1)	89.37(5)	S(1)-Cd(1)-S(1)#1	88.2(7)	S(2)-Cd(1)-S(1)	89.57(6)
S(2)-Bi(1)-S(1)#1	173.6(2)	S(1)-Cd(1)-S(1)#2	88.2(7)	S(2)#5-Cd(1)-S(1)#2	176.8(10)
S(2)#5-Bi(1)-S(1)#1	89.37(5)	S(1)#1-Cd(1)-S(1)#2	88.2(7)	S(2)#5-Cd(1)-S(2)	92.6(7)
S(2)#1-Bi(1)-S(1)	173.6(2)	S(2)-Cd(1)-S(1)#2	89.57(6)	S(2)#1-Cd(1)-S(2)#5	92.6(7)
S(2)#1-Bi(1)-S(1)#2	89.37(5)	S(2)#1-Cd(1)-S(1)#1	89.57(6)	S(2)#1-Cd(1)-S(2)	92.6(7)
Bi(1)#6-S(1)-Bi(1)#7	94.07(12)	Bi(1)#9-S(1)-Bi(1)#10	94.07(12)	Cd(1)-S(1)-Bi(1)#7	92.9(3)
Bi(1)#8-S(1)-Bi(1)	180	Bi(1)#10-S(1)-Bi(1)	85.93(12)	Bi(1)-S(2)-Bi(1)#11	94.96(16)
Bi(1)#7-S(1)-Bi(1)	94.07(12)	Bi(1)#9-S(1)-Bi(1)#6	180	Bi(1)-S(2)-Bi(1)#10	94.96(16)
Bi(1)#8-S(1)-Bi(1)#9	85.93(12)	Bi(1)#8-S(1)-Bi(1)#7	85.93(12)	Bi(1)#10-S(2)-Bi(1)#11	94.96(16)
Bi(1)#8-S(1)-Bi(1)#6	94.07(12)	Bi(1)#6-S(1)-Bi(1)#10	85.93(12)	Bi(1)#10-S(2)-Cd(1)	93.8(3)
Bi(1)#9-S(1)-Bi(1)#7	85.93(12)	Cd(1)-S(1)-Bi(1)#6	87.1(3)	Bi(1)-S(2)-Cd(1)	1.7(6)
Bi(1)#6-S(1)-Bi(1)	85.93(12)	Cd(1)-S(1)-Bi(1)#10	87.1(3)	Bi(1)#11-S(2)-Cd(1)	93.8(3)
Bi(1)#10-S(1)-Bi(1)#7	180.00(17)	Cd(1)-S(1)-Bi(1)	1.5(5)		
Bi(1)#8-S(1)-Bi(1)#10	94.07(12)	Cd(1)-S(1)-Bi(1)#9	92.9(3)		
Bi(1)#9-S(1)-Bi(1)	94.07(12)	Cd(1)-S(1)-Bi(1)#8	178.5(5)		

Symmetry transformations used to generate equivalent atoms: 1# 1+*x*,+*y*,+*z*; 2# 1+*x*,1+*y*,+*z*; 5# +*x*,-1+*y*,+*z*; 6# -1+*x*,-1+*y*,+*z*; 7# 1-*x*,-*y*,1-*z*; 8# -*x*,-*y*,1-*z*; 9# 1-*x*,1-*y*,1-*z*; 10# -1+*x*,+*y*,+*z*; 11# +*x*,1+*y*,+*z*

Table S4. Fractional atomic coordinates, equivalent isotropic displacement parameters (Å^2 × 10^3), SOFs ,and atomic sites for KCBS, *U*(eq) is defined as 1/3 of the trace of the orthogonalized U^{ij} tensor.

Compound	Atom	*x*/*a*	*y*/*b*	*z*/*c*	*U*(eq)	S.O.F	Wyckoff Position
KCBS	Bi1	2/3	1/3	0.5774(2)	10.9(4)	0.7	4*f*, 3*m*
	Cd1	2/3	1/3	0.5732(12)	10.9(4)	0.2812	4*f*, 3*m*
	S1	0	0	1/2	14.9(9)	1	2*a*, -3*m*
	S2	1/3	2/3	0.63833(16)	12.8(7)	1	4*f*, 3*m*
	K1	0.6130(30)	0.2260(60)	3/4	9(6)	0.09	6*h*, *mm*2
	K2	0.2700(190)	0.1350(90)	3/4	10(8)	0.0469	6*h*, *mm*2
	K3	0.0890(80)	0.0450(40)	3/4	10(6)	0.0898	6*h*, *mm*2

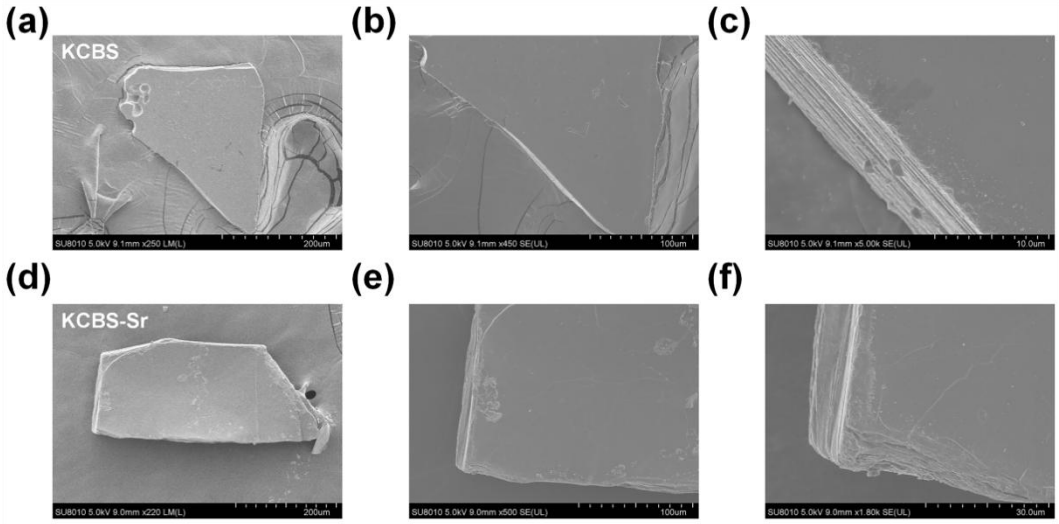


Figure S2. SEM images of (a–c) KCBS and (d–f) KCBS-Sr at different magnifications.

Table S5. Experimental results of isothermal adsorption of KCBS for Sr^{2+} (V/m = 1000 mL·g^{-1} at room temperature, 12 h contact time).

C_0^{Sr} (mg·L^{-1})	C_e^{Sr} (mg·L^{-1})	q_e^{Sr} (mg·g^{-1})
3.31 ± 0.04	0.029 ± 0.001	3.28 ± 0.04
20.16 ± 0.12	0.339 ± 0.014	19.82 ± 0.11
164.8 ± 1.9	111 ± 2	53 ± 4
239 ± 3	178.5 ± 0.4	60 ± 2
304 ± 4	242 ± 3	62 ± 7
445 ± 8	380.9 ± 0.5	64 ± 8
537 ± 10	473.1 ± 1.5	64 ± 9

Table S6. Fitting parameters of the Langmuir, Freundlich, and Langmuir-Freundlich models for the isothermal adsorption of KCBS for Sr^{2+}.

Adsorption isotherm model	Langmuir model	Freundlich model	Langmuir–Freundlich model
R^2	0.97557	0.96663	0.98396
χ^2	14.92052	20.38304	9.79757
q_m (mg·g^{-1})	60.9 ± 1.7	-	77 ± 15
b (L·mg^{-1})	1.4 ± 0.4	-	0.11 ± 0.18
n	-	5.2 ± 0.8	2.5 ± 0.7
k_F	-	21 ± 3	-

Table S7. Comparison of the adsorption capacities of KCBS with other reported materials for Sr^{2+}.

Sample	q_m^{Sr} (mg·g^{-1})	pH range	t_e^{Sr} (min)	T (K)	Ref.
KCBS	77	2-12	60	RT	This work
$Na_5Zn_{3.5}Sn_{3.5}S_{13}$	32.3	3-12	5	298	[1]
$Na_{1.60}Mg_{0.33}Sn_{3.15}S_7$	52.6	4-11	3	298	[2]
FJSM-SnS	65.19	0.7-12.7	5	338	[3]
FJSM-SnS-2	59.41	2.5-11.9	60	RT	[4]
FJSM-KSnS	59.88	2-12	10	RT	[5]
K-TaS2	37.95	1-12	30	RT	[6]
K-NbS2	79.25	0.3-12	30	RT	[6]
InS-1	105.35	3-12	1440	RT	[7]
KTS-3	102	2-12	5	RT	[8]
$Na_2Sn_3S_7$	80	3-13	5	298	[9]
KMS-2	86.89	3-10	5	RT	[10]
SnO_2-Sb_2O_5	25.7	3-12	NC	303	[11]
AMP-PAN	16	2-12	NC	293K	[12]

*NC: not clear.

Table S8. Experimental results on the kinetics of KCBS for Sr^{2+} (V/m = 1000 mL·g^{-1}; at room temperature)

t (min)	C_t^{Sr} (mg·L^{-1})	R^{Sr} (%)
0	6.45	0.00
1	5.91	8.39
2	5.55	13.93
3	5.46	15.38
5	4.36	32.38
10	2.91	54.92
15	1.77	72.51
20	1.14	82.33
30	0.31	95.08
60	0.003	99.95
120	0.055	99.15
240	0.008	99.87
360	0.036	99.44
480	0.039	99.40

Table S9. Kinetic fitting parameters of KCBS for Sr^{2+} capture.

	k_1 (min^{-1})	k_2 ($g \cdot mg^{-1} \cdot min^{-1}$)	q_e^{Sr} ($mg\ g^{-1}$)	R^2
Pseudo-first-order model	0.081 ± 0.003	-	6.48 ± 0.07	0.99568
Pseudo-second-order model	-	0.016 ± 0.003	6.9 ± 0.2	0.96191

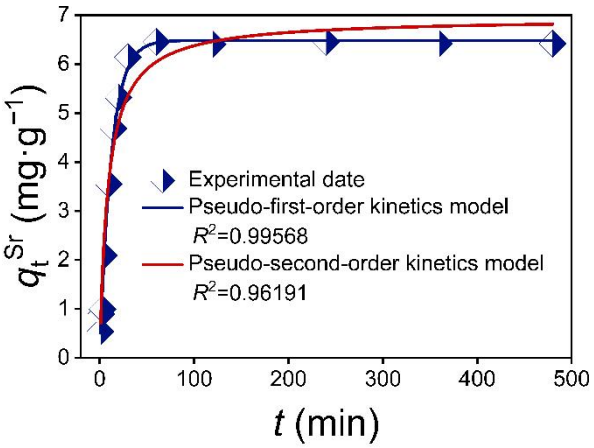


Figure S3. Pseudo-first-order kinetics model and pseudo-second-order kinetic model fitting curves for kinetic data of KCBS for Sr^{2+} capture.

Table S10. Thermodynamic parameters of Sr^{2+} adsorption by KCBS.

T (K)	K_d ($mL \cdot g^{-1}$)	ΔH^0 ($kJ \cdot mol^{-1}$)	ΔS^0 ($kJ \cdot mol^{-1} \cdot K^{-1}$)	ΔG^0 ($kJ \cdot mol^{-1}$)
293	1.01×10^4			-22.49
313	4.02×10^4	56.52	0.27	-27.88
333	1.76×10^5			-33.28

Table S11. pH-dependent adsorption results of KCBS for Sr^{2+} ions removal and leaching percentages of Cd and Bi for KCBS immersed in solutions with different pH values (V/m = 1000 $mL \cdot g^{-1}$, contact time 12 hours at room temperature).

pH	C_0^{Sr} ($mg \cdot L^{-1}$)	C_e^{Sr} ($mg \cdot L^{-1}$)	K_d^{Sr} ($mL \cdot g^{-1}$)	R^{Sr} (%)	R_L^{Bi}(%)	R_L^{Cd}(%)
2.01	3.875	2.625	4.76×10^2	32.26	0.003	0.008
2.98	5.30	0.840	5.31×10^3	84.15	0.003	0.007
4.04	3.49	0.048	7.29×10^4	98.62	0.004	0.008
4.98	4.040	0.004	1.01×10^6	99.89	0.006	0.008
6.02	3.65	0.008	4.63×10^5	99.78	0.008	0.008
7.00	3.96	0.018	2.27×10^5	99.56	0.007	0.008
8.04	3.705	0.070	5.19×10^4	98.11	0.006	0.007
8.98	3.78	0.105	3.50×10^4	97.22	0.007	0.008
10.01	3.79	0.058	6.49×10^4	98.48	0.006	0.008
11.03	3.870	0.005	7.73×10^5	99.87	0.013	0.009
12.01	3.87	0.061	6.27×10^4	98.42	0.009	0.007

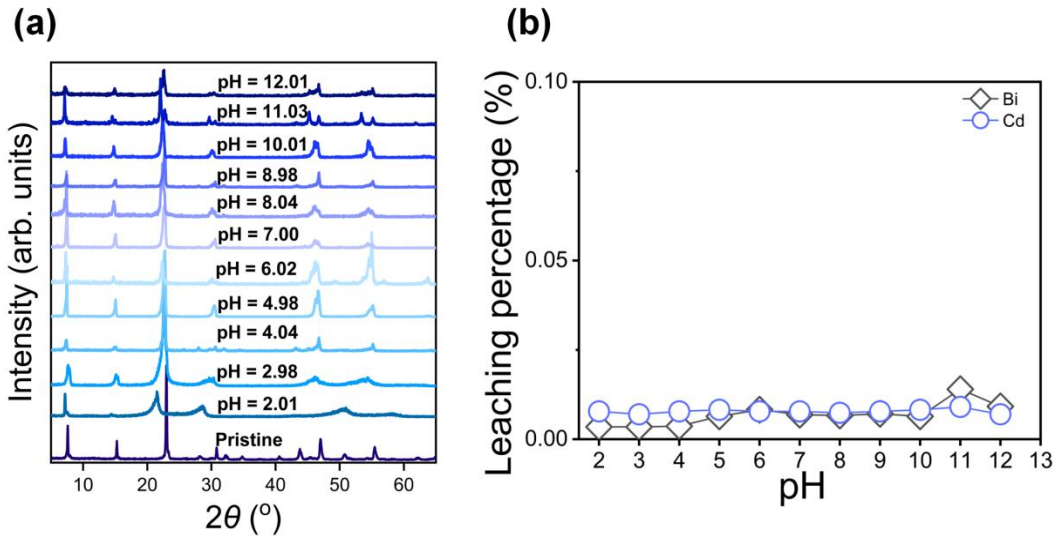


Figure S4. (a) Experimental PXRD patterns for KCBS and its corresponding samples after soaking in solutions with different pH. (b) Cd and Bi leaching percentage curves of KCBS in solutions with different pH.

Table S12. Adsorption results of KCBS under different Sr/Na molar ratios (V/m = 1000 mL·g^{-1}, at room temperature and 12 h contact time).

Molar Ratios (Sr^{2+}/Na^{+})	Sr^{2+}	C_0 (mg·L^{-1})	C_e (mg·L^{-1})	K_d (mL·g^{-1})	R (%)	$SF_{Sr/Na}$
1:7.03		5.01 ± 0.04	0.0255 ± 0.0007	$1.95 \times 10^5 \pm 4 \times 10^3$	99.491 ± 0.011	3789.77
1:43.89		3.69 ± 0.03	0.2536 ± 0.0018	$1.35 \times 10^4 \pm 6 \times 10^1$	93.13 ± 0.03	94.56
1:131.35		3.62 ± 0.04	0.28 ± 0.04	$1.19 \times 10^4 \pm 1.9 \times 10^3$	92.2 ± 1.1	100.47
1:495.79		3.71 ± 0.12	1.52 ± 0.07	$1.44 \times 10^3 \pm 1.7 \times 10^2$	59 ± 3	23.74
	Na^{+}	C_0 (mg·L^{-1})	C_e (mg·L^{-1})	K_d (mL·g^{-1})	R (%)	
		9.23 ± 0.03	8.774 ± 0.005	52 ± 3	4.9 ± 0.3	
		42.5 ± 0.6	37.2 ± 0.4	143 ± 20	12.5 ± 1.8	
		124.9 ± 1.5	111.6 ± 1.2	119 ± 14	10.6 ± 1.1	
		482 ± 8	455 ± 5	61 ± 20	6 ± 2	

Table S13. The Sr^{2+} adsorption results of KCBS under different Sr/Na/Cs molar ratios (V/m = 1000mL·g^{-1}, at room temperature and 12 h contact time).

Molar Ratios (Sr^{2+}/Cs^{+}/Na^{+})		C_0 (mg·L^{-1})	C_e (mg·L^{-1})	K_d (mL·g^{-1})	R (%)
1:2.32:72.30	Sr^{2+}	2.42 ± 0.03	0.243 ± 0.003	$8.95 \times 10^3 \pm 5 \times 10^1$	89.95 ± 0.05
	Cs^{+}	8.50 ± 0.13	2.17 ± 0.02	$2.91 \times 10^3 \pm 4 \times 10^1$	74.4 ± 0.2
	Na^{+}	45.8 ± 0.9	44.3 ± 0.5	35 ± 30	3 ± 3
1:4.69:137.94	Sr^{2+}	2.31 ± 0.04	0.837 ± 0.014	$1.76 \times 10^3 \pm 4 \times 10^1$	63.7 ± 0.6
	Cs^{+}	16.43 ± 0.16	7.72 ± 0.11	$1.13 \times 10^3 \pm 5 \times 10^1$	53 ± 1
	Na^{+}	83.6 ± 0.3	81.98 ± 0.17	19.8 ± 1.6	1.16 ± 0.16

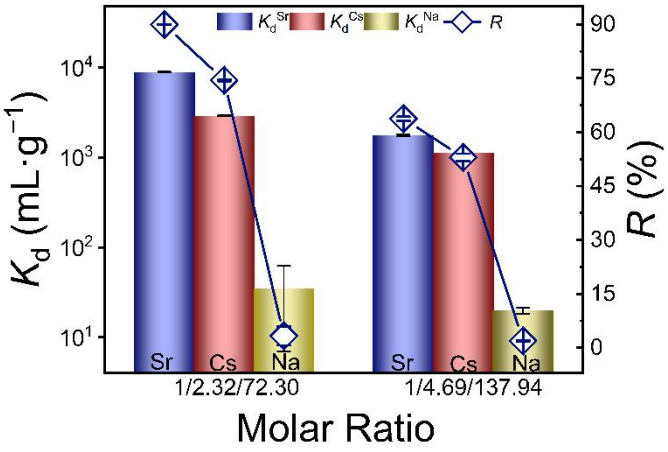


Figure S5. K_d (mL·g^{-1}) (column) and R (%) (dotted line plot) of KCBS for Sr^{2+}, Cs^{+} and Na^{+} capture in solutions with different Sr/Na/Cs molar ratios.

Table S14. Adsorption results of KCBS under different Sr/Mg molar ratios (V/m = 1000 mL·g^{-1}, at room temperature and 12 h contact time).

Molar Ratios (Sr^{2+}/Mg^{2+})	Sr^{2+}	C_0 (mg·L^{-1})	C_e (mg·L^{-1})	K_d (mL·g^{-1})	R (%)	$SF_{Sr/Mg}$
1:11.06		2.2 ± 0.6	0.0849 ± 0.0012	$2.53 \times 10^4 \pm 6 \times 10^3$	96.0 ± 1.1	5.27
1:19.17		2.264 ± 0.006	0.288 ± 0.007	$6.87 \times 10^3 \pm 1.7 \times 10^2$	87.3 ± 0.3	8.05
1:43.77		2.46 ± 0.12	1.3 ± 0.3	993 ± 300	49 ± 9	3.69
	Mg^{2+}	C_0 (mg·L^{-1})	C_e (mg·L^{-1})	K_d (mL·g^{-1})	R (%)	
		6.87 ± 0.08	1.18 ± 0.03	$4.81 \times 10^3 \pm 1.6 \times 10^2$	82.8 ± 0.5	
		12.0 ± 0.7	6.50 ± 0.12	853 ± 140	46 ± 4	
		29.87 ± 0.03	23.54 ± 0.18	269 ± 8	21.2 ± 0.5	

Table S15. Adsorption results of KCBS under different Sr/Ca molar ratios (V/m = 1000 mL·g^{-1}, at room temperature and 12 h contact time).

Molar Ratios (Sr^{2+}/Ca^{2+})	Sr^{2+}	C_0 (mg·L^{-1})	C_e (mg·L^{-1})	K_d (mL·g^{-1})	R (%)	$SF_{Sr/Na}$
1:3.54		2.394 ± 0.011	0.0283 ± 0.0009	$8.38 \times 10^4 \pm 3 \times 10^3$	98.82 ± 0.04	1.01
1:5.64		2.34 ± 0.05	1.016 ± 0.005	$1.31 \times 10^3 \pm 4 \times 10^1$	56.6 ± 0.8	1.33
1:9.95		2.428 ± 0.014	1.56 ± 0.03	559 ± 30	35.8 ± 1.4	1.46
	Ca^{2+}	C_0 (mg·L^{-1})	C_e (mg·L^{-1})	K_d (mL·g^{-1})	R (%)	
		3.87 ± 0.19	0.047 ± 0.005	$8.30 \times 10^4 \pm 1.4 \times 10^4$	98.79 ± 0.19	
		6.0 ± 0.4	3.05 ± 0.10	984 ± 60	49.6 ± 1.4	
		11.05 ± 0.14	8.00 ± 0.18	382 ± 40	28 ± 2	

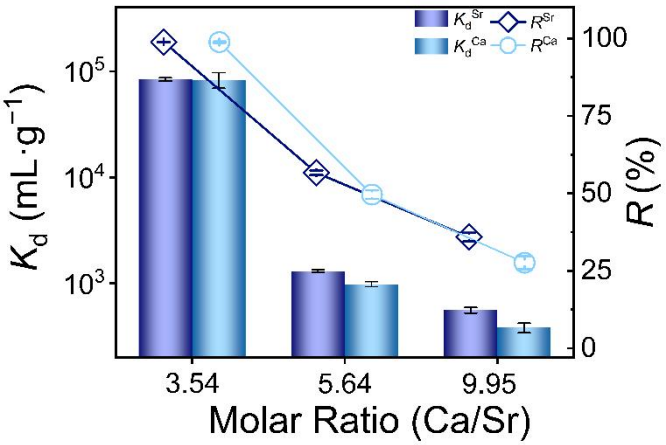


Figure S6. K_d (mL·g^{-1}) (column) and R (%) (dotted line plot) of KCBS for Sr^{2+} and Ca^{2+} capture in solutions with different Ca/Sr molar ratios.

Table S16. Adsorption results of Sr^{2+} by KCBS under coexisting conditions of Sr/Na/Cs/Mg/Ca (V/m = 1000 mL·g^{-1}, at room temperature and 12 h contact time).

Molar Ratios ($Sr^{2+}/Na^+/Cs^+/Mg^{2+}/Ca^{2+}$)		C_0 (mg·L^{-1})	C_e (mg·L^{-1})	K_d (mL·g^{-1})	R (%)
1:75.82:2.27:6.97:3.16	Sr^{2+}	2.35 ± 0.03	0.776 ± 0.015	$2.03 \times 10^3 \pm 6 \times 10^1$	67.0 ± 0.7
	Na^+	46.8 ± 0.5	45.5 ± 1.3	30 ± 18	2.8 ± 1.7
	Cs^+	8.11 ± 0.15	4.97 ± 0.11	631 ± 50	38.6 ± 1.9
	Mg^{2+}	4.54 ± 0.06	2.83 ± 0.05	605 ± 16	37.7 ± 0.6
	Ca^{2+}	3.40 ± 0.18	1.2 ± 0.1	$1.96 \times 10^3 \pm 4 \times 10^2$	66 ± 5

Table S17. The results on Sr^{2+} ions removal by KCBS in actual water samples contaminated with Sr^{2+} ions (V/m = 1000 mL·g^{-1}, at room temperature and 12 h contact time).

	C_0^{Sr} (mg·L^{-1})	C_e^{Sr} (mg·L^{-1})	K_d^{Sr} (mL·g^{-1})	R^{Sr} (%)
Tap Water (Fuzhou , Fujian)	3.028 ± 0.008	0.101 ± 0.001	$2.91 \times 10^4 \pm 3 \times 10^2$	96.68 ± 0.03
River Water (Wulong River, Fuzhou, Fujian)	3.099 ± 0.02	0.0830 ± 0.0005	$3.62 \times 10^4 \pm 2 \times 10^2$	97.315 ± 0.016
Lake Water (Qishan Lake, Fuzhou, Fujian)	3.139 ± 0.013	1.638 ± 0.013	916 ± 20	47.8 ± 0.6
Sea Water (Dongshan Islan, Zhangzhou, Fujian)	3.43 ± 0.02	1.541 ± 0.014	$1.22 \times 10^3 \pm 3 \times 10^1$	55.0 ± 0.6

Table S18. The results on Sr^{2+} ions removal by the KCBS before and after γ- and β-irradiated samples (V/m = 1000 mL·g^{-1}, at room temperature and 12 h contact time).

	C_0^{Sr} (mg·L^{-1})	C_e^{Sr} (mg·L^{-1})	K_d^{Sr} (mL·g^{-1})	R^{Sr} (%)
Pristine	8.07 ± 0.06	0.034 ± 0.003	$2.36 \times 10^5 \pm 2 \times 10^4$	99.57 ± 0.04
100 kGy β	8.07 ± 0.06	0.046 ± 0.003	$1.74 \times 10^5 \pm 1.2 \times 10^4$	99.43 ± 0.04
200 kGy β	8.07 ± 0.06	0.021 ± 0.002	$3.92 \times 10^5 \pm 5 \times 10^4$	99.74 ± 0.03
100 kGy γ	8.07 ± 0.06	2.88 ± 0.06	$1.80 \times 10^3 \pm 6 \times 10^1$	64.3 ± 0.8
200 kGy γ	8.07 ± 0.06	2.977 ± 0.018	$1.71 \times 10^3 \pm 2.0 \times 10^1$	63.1 ± 0.3

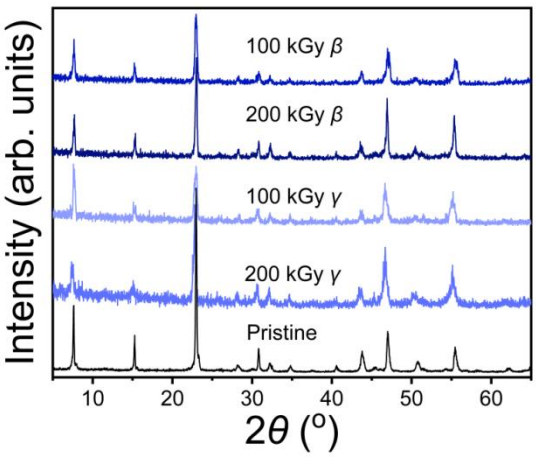


Figure S7. PXRD patterns of KCBS samples before and after β and γ irradiations.

Table S19. Results of cycling experiments.

Number of cycles	Adsorption					Desorption			
	m_1 (mg)	V_1 (mL)	C_0^{Sr} (mg·L^{-1})	C_e^{Sr} (mg·L^{-1})	R^{Sr} (%)	m_2 (mg)	V_2 (mL)	C_e^{Sr} (mg·L^{-1})	E^{Sr} (%)
1	130	130	7.9	0.0044	99.94	110	110	8.03	101.55
2	90	90	7.9	0.00135	99.98	80	80	7.77	98.21
3	50	50	7.9	0.0027	99.97	40	40	7.91	100.04

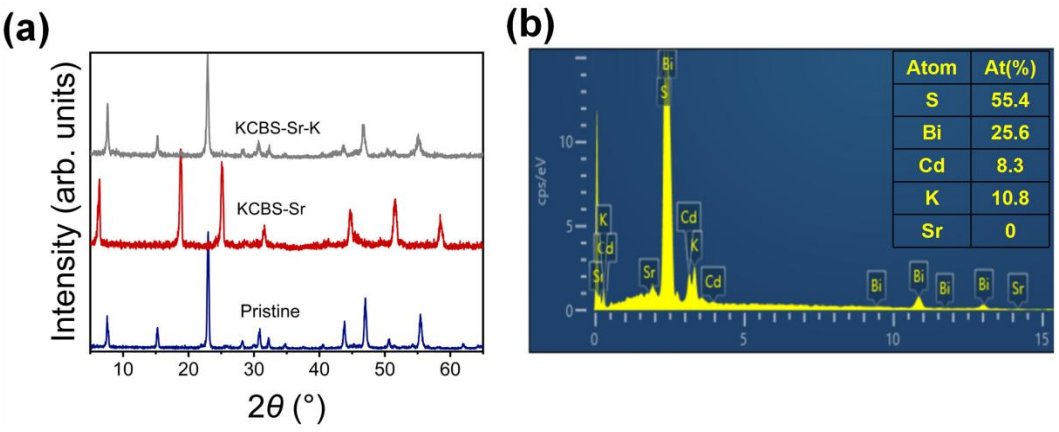


Figure S8. (a) PXRD patterns of KCBS, KCBS-Sr, and KCBS-Sr-K. (b) EDS analysis results of KCBS-Sr-K.

References

1. Zhang, M.D.; Gu, P.; Yan, S.; Dong, L.H.; Zhang, G.H. Na/Zn/Sn/S (NaZTS): Quaternary metal sulfide nanosheets for efficient adsorption of radioactive strontium ions. *Chem. Eng. J.* **2020**, 379, 122227. https://doi.org/10.1016/j.cej.2019.122227
2. Chen, Y.; Wang, Z.X.; Liu, S.R.; Zhang, G.H.; Dong, L.H.; Gu, P.; Hou, L.A. Layered metal sulfide NMTS for rapid removal of radioactive strontium ions from aqueous solution. *Sep. Purif. Technol.* **2023**, 310, 122887. https://doi.org/10.1016/j.seppur.2022.122887
3. Qi, X.H.; Du, K.Z.; Feng, M.L.; Li, J.R.; Du, C.F.; Zhang, B.; Huang, X.Y. A two-dimensionally microporous thiostannate with superior Cs^{+} and Sr^{2+} ion-exchange property. *J. Mater. Chem. A* **2015**, 3, 5665-5673. https://doi.org/10.1039/c5ta00566c
4. Li, W.A.; Li, J.R.; Zhang, B.; Sun, H.Y.; Jin, J.C.; Huang, X.Y.; Feng, M.L. Layered Thiostannates with Distinct Arrangements of Mixed Cations for the Selective Capture of Cs^{+}, Sr^{2+}, and Eu^{3+} Ions. *ACS Appl. Mater. Interfaces* **2021**, 13, 8, 10191-10201. https://doi.org/10.1021/acsami.0c22690
5. Ren, Y.W.; Luo, J.H.; Chen, Z.H.; Liu, S.Z.; Guo, X.P.; Chen, G.Y.; Feng, M.L.; Huang, X.Y. The efficient removal of Sr^{2+} using two thiostannates via ion exchange. *Dalton Trans.* **2025**, 54, 15055-15061. https://doi.org/10.1039/d5dt01904d
6. Wei, C.; Jia, S.Q.; Zhao, Y.Y.; Liu, J.T.; Sun, H.Y.; Feng, M.L.; Huang, X.Y. Efficient capture of Cs^{+} and Sr^{2+} by layered thioniobates and thiotantalate and insight into the structure-property relationship. *Sci. China Chem.* **2025,** 68, 4856-4866. https://doi.org/10.1007/s11426-025-2614-x
7. Wang, K.Y.; Sun, M.; Ding, D.; Liu, H.W.; Cheng, L.; Wang, C. Di-lacunary $[In_6S_{15}]^{12-}$ cluster: the building block of a highly negatively charged framework for superior Sr^{2+} adsorption capacities. *Chem. Commun.* **2020**, 56, 3409-3412. https://doi.org/10.1039/d0cc00441c
8. Sarma, D.; Islam, S.M.; Subrahmanyam, K.S.; Kanatzidis, M.G. Efficient and selective heavy metal sequestration from water by using layered sulfide $K_{2x}Sn_{4-x}S_{8-x}$ (x = 0.65-1; KTS-3). *J. Mater. Chem. A* **2016**, 4, 16597-16605. https://doi.org/10.1039/c6ta06404c
9. Zhang, Z.G.; Gu, P.; Zhang, M.D.; Yan, S.; Dong, L.H.; Zhang, G.H. Synthesis of a robust layered metal sulfide for rapid and effective removal of Sr^{2+} from aqueous solutions. *Chem. Eng. J.* **2019**, 372, 1205-1215. https://doi.org/10.1016/j.cej.2019.04.193
10. Mertz, J.L.; Fard, Z.H.; Malliakas, C.D.; Manos, M.J.; Kanatzidis, M.G. Selective Removal of Cs^{+}, Sr^{2+}, and Ni^{2+} by $K_{2x}Mg_xSn_{3-x}S_6$ (x = 0.5-1) (KMS-2) Relevant to Nuclear Waste Remediation. *Chem. Mater.* **2013**, 25, 2116-2127. https://doi.org/10.1021/cm400699r
11. Zhang, L.; Wei, J.Y.; Zhao, X.; Li, F.Z.; Jiang, F.; Zhang, M.; Cheng, X.Z. Competitive adsorption of strontium and cobalt onto tin antimonate. *Chem. Eng. J.* **2016**, 285, 679-689. https://doi.org/10.1016/j.cej.2015.10.013
12. Paark, Y.; Lee, Y.C.; Shin, W.S.; Choi, S.J. Removal of cobalt, strontium and cesium from radioactive laundry wastewater by ammonium molybdophosphate-polyacrylonitrile (AMP-PAN). *Chem. Eng. J.* **2010**, 162, 685-695. https://doi.org/10.1016/j.cej.2010.06.026